Locking the Hydrophobic Loop 262−274 to G-Actin Surface by a Disulfide Bridge Prevents Filament Formation†

Alexander Shvetsov,‡ Runa Musib,§ Martin Phillips,‡ Peter A. Rubenstein,§ and Emil Reisler*,‡

Department of Chemistry and Biochemistry and Molecular Biology Institute, University of California, Los Angeles, California 90095, and Department of Biochemistry, College of Medicine, University of Iowa, Iowa City, Iowa 52242

Received March 13, 2002; Revised Manuscript Received May 31, 2002

ABSTRACT: Models of F-actin structure predict the importance of hydrophobic loop 262−274 at the interface of subdomains 3 and 4 to interstrand interactions in filaments. If this premise is correct, prevention of the loop conformational change—its swinging motion—should abort filament formation. To test this hypothesis, we used site-directed mutagenesis to create yeast actin triple mutant $(LC)_2CA$ (L180C/L269C/C374A). This mutation places two cysteine residues in positions potentially enabling the locking of loop 262−274 to the monomer surface via disulfide formation. Exposure of the purified mutant to oxidation catalysts resulted in an increased electrophoretic mobility of actin on SDS PAGE and a loss of two cysteines by DTNB titrations, consistent with disulfide formation. The polymerization of un-cross-linked mutant actin by $MgCl_2$ was inhibited strongly but could be restored to wild type actin levels by phalloidin and improved greatly through copolymerization with the wild-type actin. Light scattering measurements revealed nonspecific aggregation of the cross-linked actin under the same conditions. Electron microscopy confirmed the absence of filaments and the presence of amorphous aggregates in the cross-linked actin samples. Reduction of the disulfide bond by DTT restored normal actin polymerization in the presence of $MgCl_2$ and phalloidin. These observations provide strong experimental support for a critical role of the hydrophobic loop 262−274 in the polymerization of actin into filaments.

Actin filaments play a central role in force generation and contraction of muscle cells and the motility of nonmuscle cells. The detailed understanding of these processes requires the knowledge of atomic structures of actin filaments (F-actin), actin-binding proteins, and their complexes. In the absence of direct crystallographic information, the structure of F-actin has been modeled by fitting the atomic structure of the rabbit skeletal muscle α-actin monomer (G-actin) to X-ray diffraction data obtained from oriented F-actin gels (*1*). This prevalent model of F-actin structure allows also for fitting the atomic structure of yeast G-actin (PDB entry 1YAG) to the lower-resolution electron microscopy images of yeast actin filaments (*2*).

Both in the original (*1*) and the refined (*3*) models of F-actin structure, the interactions between the two filament strands and, thus, the stability of F-actin are attributed to a large extent to the postulated structural role of loop 262−274 in actin. In G-actin this loop and its hydrophobic plug (residues 266−269), which are located between subdomains 3 and 4, are parked along subdomain 4, parallel to the longitudinal monomer axis (*4*). According to structural models of F-actin (*1, 3*), this loop swings away from the monomer surface during actin polymerization, inserting the hydrophobic plug into a hydrophobic pocket at the interface between two adjacent monomers in the opposite strand. Such a mechanism falls into a more general category of protein assemblies in which subunits and protomers share domains and loops to form higher order structures (*5*). This potential motion of the hydrophobic loop, or at least its detachment from the G-actin surface, could be deduced also from normal-mode analysis of actin structure (*6*). The detachment of the loop and its insertion into the opposite strand has been questioned, however, on grounds of an energetic barrier to such transitions in the β-actin ribbon structure (*7*). It is also possible that loop detachment, without full extension, is needed for the conformational change that makes the monomer polymerization-competent, even if the perpendicular extension is not necessary for filament stability.

Experimental testing of the hydrophobic plug hypothesis to date has involved the use of mutational substitutions of the loop residues in yeast actin to alter the hydrophobicity of the plug or to introduce sites for the attachment of fluorescent probes. The S265C (SC) mutant, with Ser-265 replaced by cysteine, enabled the simultaneous labeling of both Cys-265 and Cys-374 with pyrene maleimide, resulting in the formation of a strong excimer fluorescence band in F-actin, but not in G-actin (*8*). However, given the size of the pyrene reagent, this result provided insufficient con-

† This work was supported by grants from the USPHS (AR 22031) and NSF MCB 9904599 to E.R. and from the USPHS (GM 33689) to P.A.

* Corresponding author. Phone: (310) 825-2668. Fax: (310) 206-7286. E-mail: reisler@mbi.ucla.edu.

‡ University of California, Los Angeles.

§ University of Iowa.

[1] Abbreviations: DNase I, deoxyribonuclease I; F-actin, filamentous actin; G-actin, monomer actin; S1, myosin subfragment 1; BeFx, beryllium fluoride; DTNB, 5,5′-dithio-bis(2-nitrobenzoic acid); DTT, dithiothreitol.

10.1021/bi020205f CCC: $22.00
Published on Web 08/07/2002

straints on the distance (≤18 Å) (*9*) between Cys-265 and Cys-374 on opposite strand monomers to prove the swinging of the loop. The results of polymerization studies of the GG yeast actin mutant, in which glycine residues were substituted for the hydrophobic Val-266 and Leu-267, were consistent with the proposed role of the hydrophobic plug in filament stabilization. This actin mutant does not form filaments under normal polymerization conditions (*10*), but its assembly can be rescued by several factors, including phalloidin, BeF_x, and tropomyosin (*10*, *11*). Notably, the rescue of GG-actin polymerization by BeF_x and tropomyosin, which stabilize mainly the longitudinal intrastrand interactions in F-actin, is temperature-sensitive, whereas the rescue by phalloidin, which promotes interstrand contacts in F-actin, is temperature-insensitive. These findings reveal that at a low temperature (4 °C) which decreases hydrophobic interactions, the polymerization defect of GG-actin can be corrected only by directly strengthening the interstrand interactions in F-actin.

The hypothesized structural dynamics of loop 262−274 is consistent with recent cross-linking studies of Kim et al. (*12*). These authors used yeast actin mutants to show that Cys-265 in the loop can be cross-linked by disulfide or dibromobimane to Cys-374 and Cys-41 (replacing Gln-41 in wild-type actin) on opposite strand protomers. Structural constraints imposed by these disulfide bonds reveal closer proximity of Cys-265 to the DNase I binding loop and the C-terminus of opposite strand actins than predicted by the Holmes et al. (*1*) and Lorenz et al. (*3*) models of F-actin structure. While these constraints can be reconciled with the above models by assuming dynamic motions of the three structural elements, the disulfide bonds would not be allowed if subdomains 3 and 4 of actin were distal from the filament axis (*7*).

For the loop sharing model to be correct, it must first be rigorously demonstrated that the loop can detach from the monomer surface. Then, it must be directly demonstrated that the tip of the loop inserts into the cross-strand hydrophobic pocket. Although results of previous studies with yeast actin mutants provide support for the role of hydrophobic loop sharing in F-actin stabilization, they fall short of proving that this is a necessary condition for filament formation. To obtain direct evidence for the proposed loop behavior, we have addressed in this paper the question of loop detachment. We created yeast actin mutant $(LC)_2CA$ (i.e., L180C/L269C/C374A, with Leu-180 and Leu-269 substituted to cysteines and Cys-374 to alanine) that enables reversible locking of the loop at the monomer surface via a disulfide bridge between residues 180 and 269. We show that the disulfide cross-linked mutant actin forms amorphous aggregates while normal filaments are formed with the reduced actin.

MATERIALS AND METHODS

Materials. The site-directed mutagenesis kit was purchased from Stratagene Corp. (La Jolla, CA). Integrated DNA Technologies, Inc. (Coralville, IA) synthesized the oligodeoxyribonucleotides used for site-directed mutagenesis. Peptone, tryptone, and yeast extract were from Difco (Detroit, MI). DNase I Grade D was purchased from Worthington Biochemical Corporation (Lakewood, NJ). ATP, DTE, dithionitrobenzoic acid (DTNB), and phalloidin were obtained from Sigma Chemical Company (St. Louis, MO).

Site-Directed Mutagenesis. Site-directed mutagenesis, employing the Stratagene QuikChange mutagenesis kit, was used to construct a mutant actin sequence carried in a centromeric plasmid pRS314 (*13*) marked with the *TRP1* gene. The oligodeoxynucleotide used to generate the mutation $L_{180}C$ in $L_{269}C/C_{374}A$ actin was 5′-GAGAATCGAT-**TGT**GCCGGTAGAG-3′, and the mutant codon is underlined. The DNA was sequenced to verify the presence of the mutation by the DNA Sequencing Facility at the University of Iowa.

Yeast Transformation. The plasmid pRS314 containing the mutant actin coding sequence was introduced into a *trp1*, *ura3*−*52 Saccharomyces cerevisiae* haploid cell in which the chromosomal *ACT1* gene had been disrupted by replacement of the coding sequence with the *LEU2* gene. Wild-type actin was expressed in these recipient cells from another centromeric plasmid containing the *URA3* gene. Following transformation with the mutant plasmid and selection on tryptophan-deficient medium, surviving cells were subjected to plasmid shuffling to eliminate the plasmid carrying the WT actin gene. The mutant plasmid was rescued from surviving trp^+, ura^- cells and sequenced to ensure that the mutation was still intact. Viable cells were readily obtained.

Preparation of Proteins. Yeast actin was purified by affinity chromatography on a DNase I column as described before (*14*). To avoid a possible contamination of yeast actin with cofilin, the DNase I column was washed with 1.0 M NaCl (*15*) in 10 mM Tris-HCl (pH 7.8), 2.0 mM DTT, 0.2 mM ATP, and 0.2 mM $CaCl_2$ prior to the elution of yeast actin. The mutant actin eluted from the column migrated as a single protein band on SDS PAGE and did not require additional purification by a cycle of polymerization and depolymerization. Such cycling would have reduced greatly the yield because of polymerization inhibition. Myosin subfragment 1 (S1) was prepared according to the method of Weeds and Pope (*16*).

Disulfide Cross-linking of G-actin. Purified G-actin was stored on ice in 10 mM Tris-HCl (pH 8.0), 0.2 mM $CaCl_2$, 0.2 mM ATP, and 1.0 mM DTT, which was added on a daily basis. Prior to disulfide cross-linking reactions, DTT was removed from G-actin by passing it through a Sephadex G-50 column that was equilibrated with 10 mM MOPS buffer, pH 7.0, 0.2 mM $CaCl_2$, and 0.2 mM ATP. Cysteine residues 180 and 269 in 10 μM G-actin were cross-linked for 30 min on ice via disulfide bond formation. Between 10 and 50 μM $CuSO_4$ was added to the actin solution to catalyze air oxidation. After 30 min, the unreacted cysteine groups were blocked with 1 mM *N*-ethylmaleimide. Cross-linked actin was identified by SDS PAGE (*17*) under nonreducing conditions. The un-cross-linked and cross-linked actins have different electrophoretic mobility and can be easily resolved on these gels.

DTT Reversal of Disulfide Cross-linking in G-actin. The C180−C269 disulfide bond in G-actin was reduced by overnight incubation of the cross-linked protein on ice with 10 mM DTT in 10 mM MOPS buffer, pH 8.0, 0.2 mM $CaCl_2$, and 0.2 mM ATP.

Thiol Titration with DTNB. The reactive sulfhydryl groups on actin were titrated with DTNB under nondenaturing conditions. Actin samples (2.0 mL) containing between 5 and 100 μM −SH groups were mixed with 0.1 mL of buffer (1.0 M Tris, 1.0 M phosphate, pH 8.1) and 0.5 mL DTNB

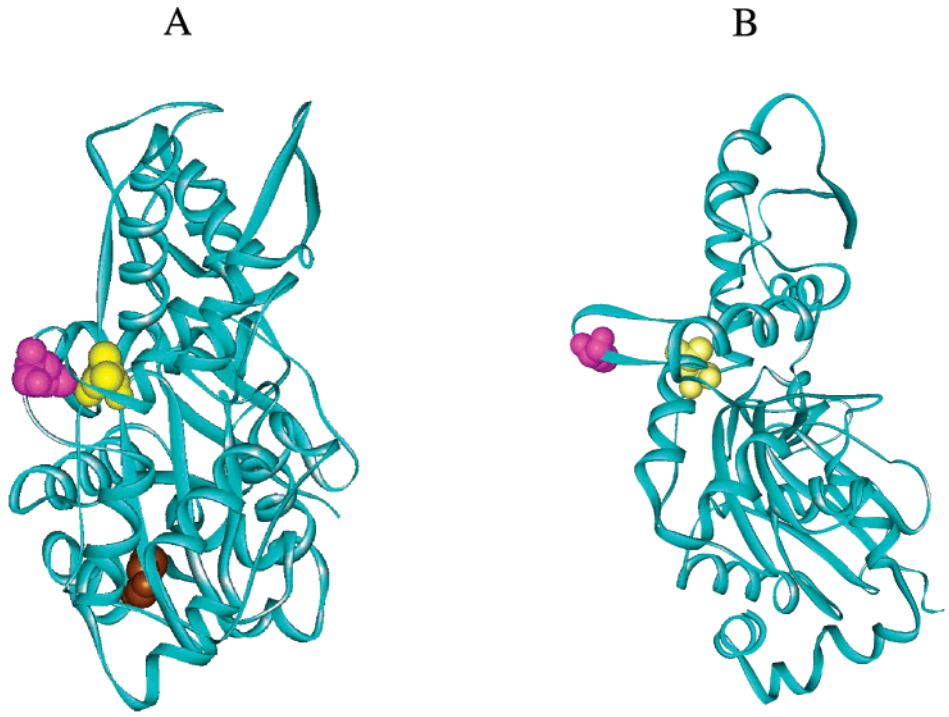

FIGURE 1: Ribbon representation of actin structure. (A) Side view of yeast G-actin structure (PDB entry 1YAG). (B) Side view of actin protomer in the Holmes et al. (*1*) model of F-actin structure. The mutated residues, L180, L269, and C374 are shown in yellow, purple, and brown space filling representation, respectively. The mutant cysteines 180 and 269 were disulfide cross-linked by oxidation.

(2.0 mM). After 30 min, the liberated thionitrobenzoic acid (TNB) was measured by absorbance at 412 nm. The number of SH groups reacted with DTNB was calculated using the molar extinction coefficient of 14,150 for TNB.

Differential Scanning Calorimetry. Actin melting experiments were carried out using a CSC 6100 Nano II Differential Scanning Calorimeter (Calorimetry Sciences Corp., Provo, UT). These measurements were perfomed on 23 μM actin in 10 mM HEPES, pH 7.2, 0.2 mM $CaCl_2$, and 0.2 mM ATP, at a heating rate of 1 °C/min

Actin Polymerization Assays. Actin polymerization was monitored via light scattering measurements in a SPEX Fluorolog spectrofluorometer (Jobin Yvon Inc., Edison, NJ) set at 325 nm for both the excitation and emission wavelengths. The polymerization was induced by adding 3.0 mM $MgCl_2$ and, when present, equimolar amounts of phalloidin to 10 μM G-actin in 10 mM MOPS buffer (pH 8.0), 0.2 mM $CaCl_2$, and 0.2 mM ATP. When indicated, actin was polymerized by the addition of 2.0 mM $MgCl_2$ and 50 mM KCl, or equimolar amounts of S1, to G-actin solutions. Disulfide cross-linked and un-cross-linked G-actin was polymerized in the absence and presence of 1.0 mM DTT, respectively.

Electron Microscopy. Samples of actin freshly polymerized with 3.0 mM $MgCl_2$ and equimolar amounts of phalloidin were diluted with the polymerizing buffer to 2.5 μM immediately before spreading on carbon-coated grids and negatively stained with uranyl acetate. S1, when present, was added at 1:1 molar ratio to actin. Mixtures of S1 and polymerized actin were incubated for 30 min prior to grid preparation. In the assays of actin polymerization, S1 was added to the reduced and oxidized $(LC)_2$CA G-actin. These mixtures were then incubated for 1 h at room temperature to allow for actin polymerization prior to grid preparation. The preparation of electron microscopy grids followed the previously reported procedure (*18*).

RESULTS

Blocking the motion of loop 262−274 should provide a rigorous test for the hypothesis that its detachment from the surface of the actin monomer is required for actin polymerization. This goal could be potentially achieved through engineering cysteine residues into the loop and the adjacent surface peptide, thereby enabling their reversible disulfide cross-linking. Inspection of the atomic structure of yeast G-actin (PDB entry 1YAG) and the model of F-actin structure (*1*) revealed that Leu-269 in the loop and Leu-180 at the monomer surface would be appropriate candidates for such a disulfide cross-linking (Figure 1A,B). To avoid complications resulting from a possible cross-linking of Cys-374 to Cys-269 in the mutant actin, we also replaced C-374 with alanine to yield $(LC)_2$CA (L180C/L269C/C374A) actin.

Reversible Disulfide Cross-linking of $(LC)_2$CA Actin. Copper-catalyzed air oxidation of $(LC)_2$CA G-actin resulted in its complete transformation, after 30 min on ice, into a species with a higher electrophoretic mobility on SDS PAGE than that of untreated actin (Figure 2A). Similar treatment of wild-type and rabbit skeletal actin had no effect on their migration on SDS gels (Figure 2A). Shorter incubation times produced two populations of $(LC)_2$CA actin, with the mobilities of the oxidized and unoxidized protein. Identical SDS PAGE patterns were observed also when the mutant actin was oxidized in the presence of 100 μM iodine in lieu of copper or by air alone in the absence of any catalyst. In the last case, the oxidation was completed after incubation for 2 or 3 days on ice (data not shown). Several attempts to cross-link Cys-180 to Cys-269 in G-actin by dibromobimane

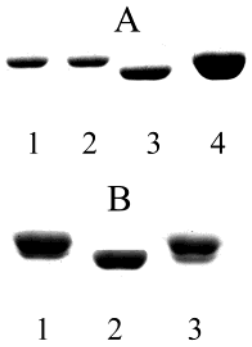

FIGURE 2: SDS PAGE patterns of $(LC)_2CA$ actin. (A) G-actin: 1, oxidized wild-type yeast actin; 2, un-cross-linked $(LC)_2CA$ actin; 3, oxidized, disulfide cross-linked $(LC)_2CA$ actin; 4, oxidized skeletal α-actin. (B) $(LC)_2CA$ F-actin: 1, un-cross-linked actin; 2, oxidized, disulfide cross-linked actin; 3, the sample shown in lane 2 after cross-linking reversal by 10 mM DTT. Actin oxidation and reduction were carried out as described in Materials and Methods.

Table 1: Free SH Groups on Actin Determined from DTNB Titrations

actin	SH/actin
wild type	1.1 ± 0.2
$(LC)_2$ CA	
reduced	2.0 ± 0.4
oxidized	0.3 ± 0.2
oxidized-DTT treated	1.9 ± 0.3

(DBB), which has an average cross-linking span of 4.9 Å (*19*) failed to produce any detectable amounts of higher mobility (cross-linked) actin on SDS PAGE.

Less expected was the formation of a disulfide bond in phalloidin-stabilized mutant F-actin, oxidized under similar conditions in the presence of copper. According to the Holmes et al. (*1*) model of F-actin structure, the thiol groups on Cys-180 and Cys-269 may be separated in the filament by close to 10 Å, as opposed to ∼5.9 Å in G-actin. The migration on SDS PAGE of actin oxidized in F- and G-actin forms was identical (Figure 2B).

Because disulfide cross-linking is reversible, we examined the recovery of the "native" form of the oxidized actin upon its incubation with DTT. After overnight treatment with DTT, most of the oxidized actin (= 90%) reverted to the reduced form as judged by its migration on SDS gels (Figure 2B). Shorter incubations of the cross-linked $(LC)_2CA$ actin with DTT resulted in its incomplete conversion into reduced actin, as reflected in the presence of the fast and slow migrating actin bands on SDS gels.

To confirm our interpretation of SDS PAGE patterns of $(LC)_2CA$ actin, the free thiol groups on actin were titrated with DTNB (Table 1). Both the untreated (reduced) and the oxidation-reversed (oxidized and then reduced) $(LC)_2CA$ actin showed close to 2.0 free thiol groups in such titrations. Only 0.3 ± 0.2 thiol groups were detected by DTNB in the oxidized actin (Table 1). These data support the conclusion that oxidation of $(LC)_2CA$ actin results in reversible disulfide cross-linking of Cys-180 to Cys-269 in the mutant protein. Differential scanning calorimetry melting experiments revealed slight destabilization of $(LC)_2CA$ actin upon its disulfide cross-linking. The melting temperatures for the reduced and disulfide cross-linked actin were 59.3 and 57.3 ± 0.3 °C, respectively, with the wild-type actin melting at 60.8 ± 0.2 °C.

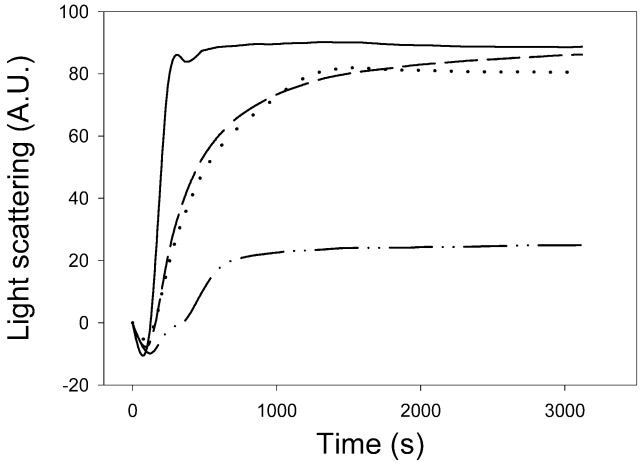

FIGURE 3: Polymerization of $(LC)_2CA$ Ca^{2+}−G-actin at 25 °C. Polymerization of actin (9.3 μM) was initiated by addition of 50 mM KCl and 2.0 mM $MgCl_2$ and was followed as a function of time using a light-scattering assay. *Solid line*, wild-type actin polymerized in the presence of equimolar phalloidin; *dashed line*, $(LC)_2CA$ actin polymerized in the presence of equimolar phalloidin; *dotted line*, wild-type actin; and *dashed*−*dotted line*, $(LC)_2CA$ actin.

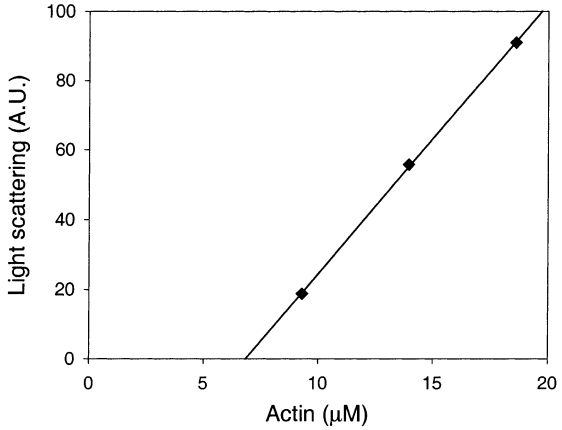

FIGURE 4: Estimation of the critical concentration for polymerization of $(LC)_2CA$ actin at 25 °C. The extent of polymerization of 9.3, 13.6, and 18.9 μM actins after reaction completion was plotted against the actin concentration. The line intercepts the *x*-axis at 6.8 μM.

Polymerization of the Reduced $(LC)_2CA$ Actin. To assess the effect of the mutations, we determined the polymerization characteristics of $(LC)_2CA$ actin. At 9.3 μM, the extent of polymerization was only 30% compared to wild-type actin at the same concentration (Figure 3, bottom vs top line). Since there was an apparent effect of the mutation on the critical concentration, we carried out the polymerization experiments at two higher actin concentrations, 13.9 μM and 18.6 μM. The light scattering was plotted as function of actin concentration and the apparent critical concentration of the mutant actin was estimated at 6.8 μM (from extrapolation of the curve in Figure 4), as compared to critical concentration of 0.41 μM for wild-type actin (*20*). Since a mutation at 269 has no apparent effect on the polymerization of L269C/C374A actin (*21*), the defect in polymerization exhibited by $(LC)_2CA$ actin is probably largely due to the mutation at position 180.

We then determined whether the filament stabilizing compound, phalloidin, or increasing amounts of copolymerized wild-type actin could overcome the polymerization defect caused by the L180 mutation. Addition of equimolar

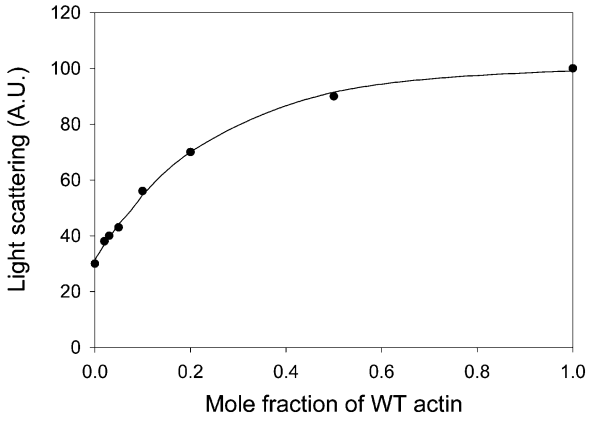

FIGURE 5: Copolymerization of Ca^{2+} wild-type and $(LC)_2CA$ actins at 25 °C at different mole ratios of the two proteins. Conditions were the same as those in Figure 3. The total actin concentration was 10 μM. Polymerization of each mole mixture of the two actins was monitored by normalizing the final light scattering values for each mixture to the light scattering for wild-type actin alone. These relative scattering values, which correspond to the extent of polymerization of each mixture, were plotted as a function of the molar fraction of wild-type actin in10 μM total actin.

phalloidin to 9.3 μM $(LC)_2CA$ actin (Figure 3, dashed line) allowed the actin to polymerize to the same extent as WT actin (Figure 3, solid line). Copolymerization of $(LC)_2CA$ actin with increasing amounts of wild-type actin is depicted in Figure 5 as the dependence of light scattering on the mole fraction of wild-type actin. Assuming that at 25 °C wild-type actin (10 μM) is fully polymerized, the 1:1 mole mixture of wild type and $(LC)_2CA$ actin (10 μM total concentration) appears ~90% polymerized. Assuming, furthermore, that all of the wild-type actin is polymerized, this result indicates that~80% of the mutant actin polymerized in this mixture. As the percent of wild type actin in the mixture decreased, the total actin that polymerized also decreased. At a wild type:mutant ratio of 1:10, approximately 50% of the total actin had polymerized.

Electron microscopy observations of $(LC)_2CA$ actin polymerized with $MgCl_2$ and phalloidin confirmed the results of light scattering experiments: the un-cross-linked actin formed standard actin filaments (Figure 6A). We observed also normal arrowhead decoration of the reduced $(LC)_2CA$ actin filaments by S1 (Figure 6B). This observation indicates that S1 binding is preserved in the reduced $(LC)_2CA$ actin. S1 polymerizes the mutant G-actin in the absence of $MgCl_2$ and phalloidin, albeit such a polymerization is slower and less complete than that with wild-type actin (data not shown). Electron microscopy images of $(LC)_2CA$ actin polymerized by S1 (Figure 6C) are similar to those observed upon addition of S1 to phalloidin-stabilized filaments (Figure 6A), but with much greater propensity of relatively short, decorated filaments.

Polymerization of the Oxidized $(LC)_2CA$ Actin. The light scattering profile of the polymerization of disulfide cross-linked $(LC)_2CA$ G-actin by $MgCl_2$ and phalloidin was strikingly different from that of wild-type actin. The light scattering increase did not appear to reach a plateau (Figure 7), suggesting a nonspecific aggregation of this actin. Reduction of the disulfide bond in $(LC)_2CA$ actin, as evidenced by SDS PAGE migration and DTNB titration, restored to a large extent the light scattering profile of the polymerization reaction to that commonly seen for actin

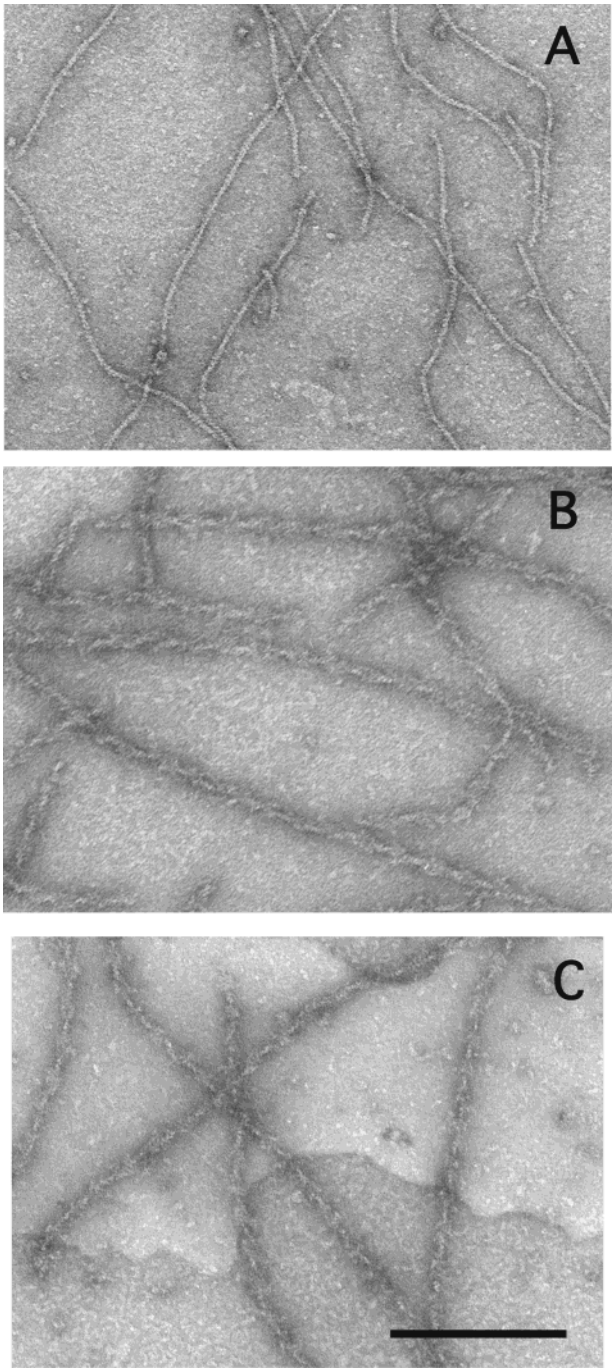

FIGURE 6: Electron micrographs of $(LC)_2CA$ actin filments. (A) Un-cross-linked actin polymerized by $MgCl_2$ and phalloidin; (B) arrowhead decoration of $(LC)_2CA$ actin filaments in (A) by S1; (C) reduced $(LC)_2CA$ G-actin polymerized by S1. Arrowhead decorated filaments are on average shorter in these fields than in panel B. All reduction and polymerization reactions were carried out on 10 μM $(LC)_2CA$ actin as described in Materials and Methods. The bar represents 2000 Å.

(Figure 7). In agreement with these light scattering results, but in contrast to the images of reduced mutant actin filaments (Figure 6A), the oxidized mutant G-actin polymerized by $MgCl_2$ and phalloidin showed only as amorphous aggregates of variable size and shape in our electron micrographs (Figure 8A). Large aggregates appearing in electron micrographs of this actin are not shown in Figure 8A because of their heavy staining. Similar aggregates, albeit with greater abundance of monomers and occasional short filaments, were present also in electron micrographs of the

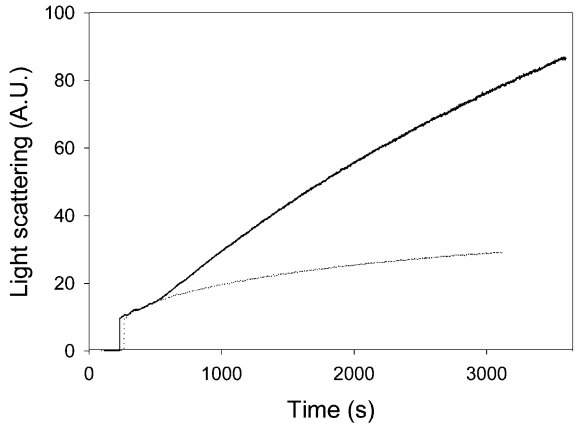

FIGURE 7: Light scattering measurements of the polymerization of disulfide cross-linked $(LC)_2CA$ actin. *Solid line*, actin (10 μM) mixed with 3.0 mM $MgCl_2$ and phalloidin; *dotted line*, cross-linked actin after overnight treatment with 10 mM DTT, mixed with 3.0 mM $MgCl_2$ and phalloidin.

oxidized $(LC)_2CA$ actin filaments (on SDS gels this actin was indistinguishable from the disulfide cross-linked G-actin; Figure 2B).

DTT reversal of disulfide cross-linking in G-actin restored its ability to form normal actin filaments in the presence of $MgCl_2$ and phalloidin (Figure 8B). SDS gel analysis and thiol titration of this actin verified the disulfide bond reduction (Figure 2A, Table 1). Similar reversal of the disulfide bond worked well also in the aggregated $(LC)_2CA$ sample containing $MgCl_2$ and phalloidin. DTT treatment of the aggregates shown in Figure 8A converted them into standard actin filaments (Figure 8C). These results demonstrate that the transition between filaments and aggregates of $(LC)_2CA$ actin in the presence of $MgCl_2$ and phalloidin is determined by the presence or absence of a disulfide lock of the conformation, position, and motion of loop 262−274 in actin.

Addition of myosin subfragment 1 (S1) to the aggregated $(LC)_2CA$ actin did not change its morphology, except for the appearance of even larger aggregates and, very infrequently, short filaments decorated by S1. S1 was unable also to polymerize the oxidized $(LC)_2CA$ G-actin, and higher-order structures were not detected in electron microscopy observations of such mixtures. Thus, like phalloidin, S1 cannot restore filament assembly for the disulfide cross-linked actin.

DISCUSSION

The goal of this study has been to test the premise of the Holmes et al. (*1*) and Lorenz et al. (*3*) models of F-actin structure that a detachment of the hydrophobic loop 262−274 from the monomer surface, and perhaps its perpendicular extension and insertion into the opposite strand of actin protomers is required for filament formation and stability. The results of several studies on the polymerization (*10, 13*) and cross-linking (*12*) of yeast actin mutants, with substitutions in the hydrophobic loop, support the loop motion hypothesis, but do not prove it, and do not show that the loop sharing is indeed necessary for filament formation. Similarly, molecular dynamics simulations of loop conformation are consistent with its release from the monomer surface (*22*), but are inconclusive regarding Schutt et al.'s (*7, 23*) suggestion that such a release would not be favored

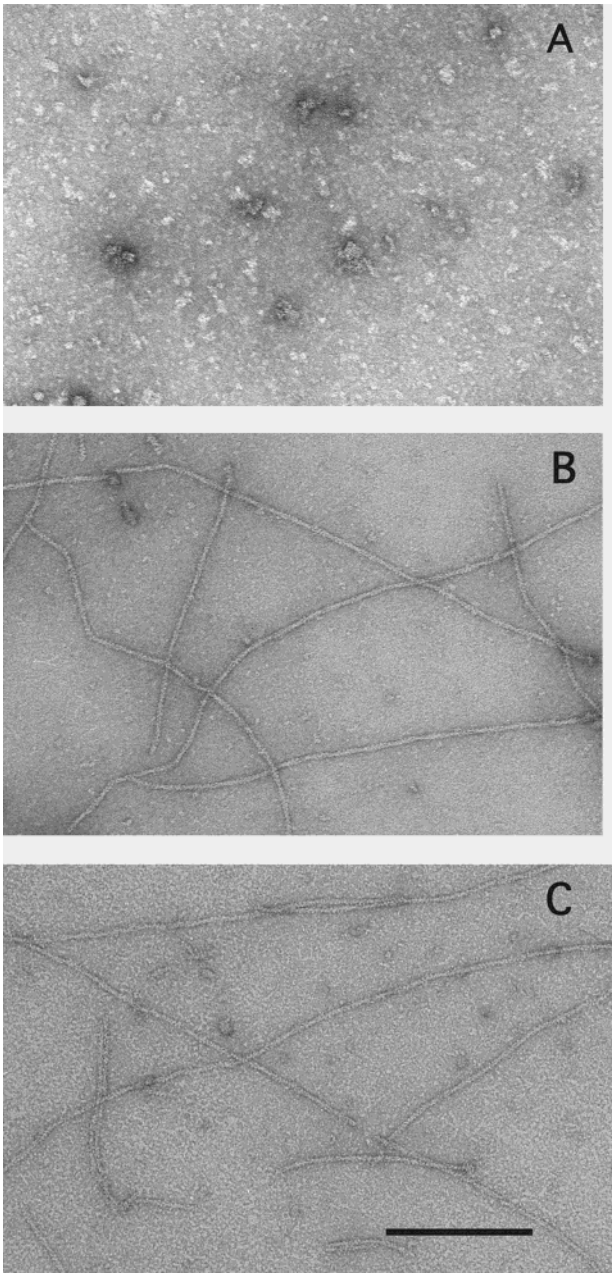

FIGURE 8: Electron micrographs of oxidized $(LC)_2CA$ actin polymerized by $MgCl_2$ and phalloidin. (A) Disulfide cross-linked actin; (B) actin polymerized after cross-linking reversal in G-actin; (C) actin after DTT treatment of aggregates of cross-linked $(LC)_2CA$ actin shown in (A). All oxidation, reduction, and polymerization reactions were carried out on 10 μM $(LC)_2CA$ actin as described in Materials and Methods. The bar represents 2000 Å.

by the salt bridge of Glu-259 and Arg-312 in their crystal structure of actin:profilin. The $(LC)_2CA$ mutant actin prepared in this work was designed to test the release aspect of the loop swapping hypothesis by the reversible, disulfide locking of the hydrophobic loop at the monomer surface.

In analogy to other loop mutants with non-hydrophobic substitutions for hydrophobic residues (*10*), the reduced $(LC)_2CA$ mutant actin shows a strongly depressed polymerization (with a high critical concentration), which can be restored to normal levels by phalloidin. Copolymerization with wild type actin rescues also to a significant extent the assembly of the mutant actin. The mutant yeast cells grow well, indicating that the polymerization defect of $(LC)_2CA$

actin is "corrected for" in the cellular environment. Clearly, if loop release from monomer surface is required for actin polymerization, it must be occurring in the $(LC)_2CA$ mutant. This result alone does not strengthen the argument for the loop motion and insertion into the opposite strand beyond that was known before. The novel aspect of the $(LC)_2CA$ mutant is that it allowed for disulfide bridging between Cys-269 in the loop and Cys-180 at the monomer surface. The quantitative formation of the disulfide bond and its virtually complete reduction by DTT were confirmed by SDS PAGE and DTNB titrations of the reduced and oxidized actin.

Electron microscopy and light scattering measurements on the reduced and disulfide cross-linked $(LC)_2CA$ actin provided striking evidence for the inability of the latter to form filaments in the presence of $MgCl_2$ and phalloidin, yielding, instead, amorphous actin aggregates of variable size. The contrast between the aggregation of oxidized actin and, after disulfide reduction, the formation of normal filaments that can be also decorated by S1 shows that loop 262−274 detachment is required for filament assembly. Perhaps the best demonstration of the critical role of loop mobility in determining the assembly pathway for actin is the DTT-induced transformation of aggregated actin into normal filaments (Figure 8C).

It is not clear whether the aggregation shown for the oxidized $(LC)_2CA$ actin represents a branch of polymerization pathway that might be present under all conditions but is not favored when the hydrophobic loop is mobile. The shift of the DTT-treated aggregates to filaments may proceed through the assembly into F-actin of reduced actin monomers that exist in the solution and the consequent, continuous reequilibration of the aggregated and dissociated actin. Alternatively, and more likely, the reduction of the disulfide bond between Cys-180 and Cys-269 may destabilize actin aggregates, creating a pool of reduced monomers for filament formation.

Interestingly, Cys-180 and Cys-269 can form also a disulfide bond in F-actin, in which the loop conformation and the distance between these cysteines should not favor such a reaction. However, we cannot rule out the possibility that it is the small fraction of monomers—present in the solution—that is preferentially oxidized, pulling the equilibrium toward filament depolymerization, and monomer oxidation and aggregation. A more likely mechanism is that of local dynamic instability within the filaments, with the hydrophobic loop fluctuating between the extended, filament-like and the collapsed, monomer-like conformation. Alternatively, the loop may be less extended in the filament than predicted in the model of F-actin structure (*1*).

Such fluctuations, as well as prior cross-linkings of Cys-265 to Cys-374 and Cys-41 to Cys-265 (*12*), may be the manifestations of dynamic behavior of the hydrophobic loop and the other structural elements on actin. The conformational instability of the loop is probably increased by substitutions of the hydrophobic residues on it and may be greater in $(LC)_2CA$ than in wild-type actin. Previous work (*10*) shows that a nonpolymerizing mutant actin, GG, in which two of the three hydrophobic residues are replaced by glycines, will polymerize in the presence of an equivalent amount of wild-type actin. This result demonstrates that at most, 50% of the residues must be capable of forming a plug pocket interaction for stable filament formation. Thus, dynamic instability of the loop is compatible with formation of stable actin filaments. It is also possible that the loop flexibility in F-actin contributes to the twist polymorphism of actin filaments (*24*, *25*) and determines, along with the DNase I binding loop and the C-terminus, the conformational states of F-actin.

REFERENCES

1. Holmes, K. C., Popp, D., Gebhard, W., and Kabsch, W. (1990) *Nature 347*, 44−49.
2. Orlova, A., Galkin, V. E., VanLoock, M. S., Kim, E., Shvetsov, A., Reisler, E., and Egelman, E. H. (2001) *J. Mol. Biol. 312*, 95−106.
3. Lorenz, M., Popp, D., and Holmes, K. C. (1993) *J. Mol. Biol. 234*, 826−836.
4. Kabsh, W., Mannherz, H. G. Suck, D., Pai, E. F., and Holmes, K. C. (1990) *Nature 347*, 37−44.
5. Bennett, M. J., Schlunegger, M. P., and Eisenberg, D. (1955) *Protein Sci. 4*, 2455−2468.
6. Tirion, M. M., ben-Avraham, D., Lorenz, M., and Holmes, K. C. (1995) *Biophys. J. 68*, 5−12.
7. Schutt, C. E., Myslik, J. C., Rozycki, M. D., Goonesekere, N. C. W., and Lindberg, U. (1993) *Nature 365*, 810−816.
8. Feng L, Kim, E., Lee, W.-L., Miller, C. J., Kuang, B., Reisler, E., and Rubenstein, P. A. (1997) *J. Biol. Chem. 272*, 16829−16837.
9. Lehrer, S. S. (1995) *Subcell. Biochem. 24*, 115−132.
10. Kuang, B., and Rubenstein, P. A. (1997) *J. Biol. Chem. 272*, 1237−1247.
11. Wen, K.-K., Kuang, B., and Rubenstein, P. A. (2000) *J. Biol. Chem. 275*, 40594−40600.
12. Kim, E., Wriggers, W., Phillips, M., Kokabi, K., Rubenstein, P. A., and Reisler, E. (2000) *J. Mol. Biol*. 299, 421−429.
13. Chen, X., Cook, R. K., and Rubenstein, P. A. (1993) *J. Cell Biol. 123*, 1185−1195.
14. Cook, R. K., Root, D., Miller, C., Reisler, E., and Rubenstein, P. A. (1993) *J. Biol. Chem*. 268, 2410−2415.
15. Du, J., and Frieden, C. (1998) *Biochemistry 37*, 13276−13284.
16. Weeds, A. G., and Pope, B. (1977) *J. Mol. Biol. 111*, 129−57.
17. Laemmli, U. K. (1970) *Nature 227*, 680−685.
18. Kim, E., Phillips, M., Hegyi, G., Muhlrad, A., and Reisler, E. (1998) *Biochemistry 37*, 17793−17800.
19. Green, N. S., Reisler, E., and Houk, K. N. (2001) *Protein Sci. 10*, 1293−1304.
20. Chen, X., and Rubenstein, P. A. (1995) *J. Biol. Chem. 270*, 11406−11414.
21. Musib, R., Wang, G., Geng, L., and Rubenstein, P. A. (2002) *J. Biol. Chem.* (in press).
22. Wriggers, W., and Schulten, K. (1999) *Proteins: Struct. Funct. Genet. 35*, 262−273.
23. Schutt, C. E., Rozycki, M. D., and Lindberg, U. (1994) *Curr. Biol. 4*, 185−186.
24. McGough, A., Pope, B., Chiu, W., and Weeds, A. (1997) *J. Cell. Biol. 138*, 771−781.
25. Galkin, V. E., Orlova, A., Lukoyanova, N., Wriggers, W., and Egelman, E. H. (2001) *J. Cell. Biol. 153*, 75−86.

BI020205F